PONTIFICIA UNIVERSIDAD CATÓLICA DEL PERÚ
FACULTAD DE CIENCIAS E INGENIERÍA

Estudio y aplicación de métodos analíticos para la extracción de parámetros eléctricos del modelo de un solo diodo para distintas tecnologías de módulos fotovoltaicos

Trabajo de investigación para obtener el grado académico de BACHILLER EN CIENCIAS CON MENCIÓN EN FÍSICA

AUTOR:
Renzo Alberto Perich Ibáñez

ASESOR:
Jan Amaru Palomino Töfflinger

Lima, Diciembre, 2020

Abstract:

The single-diode model is used to characterize a photovoltaic (PV) solar cell using an equivalent circuit and an equation that depends on five electric parameters. Three analytical methods are applied to extract the five parameters from an Aluminium Back Surface Field (Al-BSF) PV module using 500 experimental current-voltage (I-V) curves measured in the 100-1000W/m^2 range. Two of these methods are also applied to four thin-film PV modules, using four experimental I-V curves measured at an irradiance of 1000 W/m^2 and air temperature 25°C. While parameter extraction methods have been studied before, this work offers a new perspective by applying the techniques to outdoor PV modules in Lima-Peru and, on the other hand, thin-film technologies located in Jaen-Spain. Results are presented by comparing the measured I-V curve with the ones modelled using the extracted parameters. The Normalized Root Mean Square Error (NRMSE) is calculated to evaluate and compare each extraction method. Values of NRMSE are then grouped by irradiance using a series of boxplots or bar charts to better visualize the success of each extraction method. The results indicate that the method proposed by Phang et al. is very robust, obtaining low values for error across the different irradiances and technologies (median NRMSE of 0.20 % for silicon and 0.50-1.10 % for thin-films). The Blas et al. method obtained low error with the silicon module (median NRMSE of 0.21 %), it was not applied to thin-films in this study. Finally, the Khan et al. method showed greater error than the other two when applied to the Al-BSF and thin-film modules, with noticeably higher error when applied to amorphous silicon modules (median NRMSE of 0.30 % for silicon and 1.77-6.73 % for thin-films).

Contents:

Introduction

Photovoltaic modules have increasingly become a more attractive solution to tackle the ever-present global warming problem. [Jordehi 2016]. Over the past decades researchers have made advances in reducing the production costs of PV modules [Wang 2014], which also lowers the price at which they are sold. Among the other benefits of photovoltaics are the lack of greenhouse gas emissions during operation and the possibility of safely installing solar power plants in the vicinity of cities or setting up modules inside the city itself to minimize transmission losses [Ciulla 2014]. As well as dependence on the sun, which is a renewable and virtually unlimited source of power. The reasons for expanding PV research are abundant, by performing more studies our knowledge of these technologies increases and they become more predictable and reliable. This in turn reduces inversion risks and can be used to support government initiatives to increase solar energy use which can have a noticeable impact in addressing global warming.

Electric characterization improves our understanding of PV technologies and lets us know more about their advantages and disadvantages [Perich 2020]. It provides useful information that is often not included by the manufacturer, especially since the information they provide is taken at standard test conditions which are AM 1.5, 1000 W/m^2 and cell temperature 25 °C. In reality, PV modules are exposed to a wide array of environmental factors that influence power generation and degradation [Ogbomo 2017]. The focus of this study will be the extraction of electric parameters from the single-diode model to characterize a silicon-based module and four thin-film modules. These techniques have not yet been applied to the conditions found in Lima-Peru, so this work continues to expand on the knowledge of PV characterization by applying three extraction methods to a silicon-based module located in the Pontificia Universidad del Peru's physics department. The techniques presented in this study also have not been applied to

thin-film technologies before, so the results obtained will provide new insights on these technologies.

The objectives of this study were to compare and evaluate the extraction methods under different irradiances and various types of PV modules, in order to find out which one is the most consistent in successfully extracting the parameters. This was done by using each extraction method to obtain the five parameters from the experimental I-V curve measurements and using them to simulate I-V curves. The modelled curves were then compared to the experimental I-V curves, for each technology and irradiance.

Theory of the Single Diode Model

The single-diode model is used to characterize PV cells [Montes-Romero 2018]. Solving its equations provides a set of parameters which can then be used in other studies to learn more about the quality of the PV module and how it will behave in time.

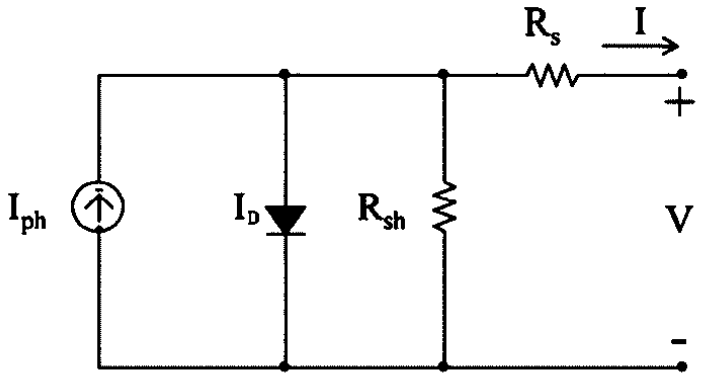

Figure 1. Equivalent circuit of a PV cell in the single-diode model [Montes-Romero 2018]

The model uses a simple electrical circuit (figure 1) to represent the physical processes which take place inside a single cell. The direct current generator represents the cell's ability to generate an electric current using incident sunlight while the diode represents the PN-junction found inside the cell. A couple of resistances, in series (R_s) and in parallel (R_{sh}), are added to take into consideration electrical losses. When applying Kirchhoff's laws to this circuit, there are three currents which must be taken into

consideration: the photocurrent (I_{ph}), the current going through the diode (I_D) and the one going through the shunt resistance (I_{sh}). The latter two currents are parasitic or losses and must be subtracted from the photocurrent generated by the cell. The diode current can be found using Shockley's diode equation, while the current associated with the shunt resistance is easily obtained by dividing the potential difference across the resistance by its value in ohms. After adding these a relationship between current and voltage is obtained [Ghani 2014], this equation features five electric parameters whose calculation based on the experimental I-V curve will be the focus of this study. The term V_t is known as the thermal voltage, it is calculated using Equation 4 where k is the Boltzmann constant, q is the elementary charge and T is the PV cell's temperature.

$$I_D = I_0(Exp[[\frac{V + I\,Rs}{n\,Vt}] - 1)] \quad (1)$$

$$I_{sh} = V + \frac{I\,R_s}{R_{sh}} \quad (2)$$

$$I = I_{ph} - I_D - I_{sh} \quad (3)$$

$$V_t = \frac{k\,T}{q} \quad (4)$$

$$I = I_{ph} - I_0(Exp\,[\frac{V + I\,R_s}{n\,V_t}] - 1\,) - \frac{V + IR_S}{R_{sh}} \quad (5)$$

The five electric parameters provide information on the physical processes going on inside the cell. The photocurrent (I_{ph}) is the current generated by the PV cell thanks to its light absorbing abilities, this is before taking into consideration resistive losses and is known to behave linearly with irradiance. The diode saturation current (I_0) represents a diffusion current and recombinations which take place in the PN-junction [Kumar 2017]. The series resistance (R_s) is mainly affected by the resistance of the electric contacts located at the top and bottom side of the cell, ideally this parameter would be equal to

zero. The parallel or shunt resistance (R_{sh}) is related to undesired leak currents which cause electrical losses [Jordehi 2016]. In an ideal cell, R_{sh} is infinite. Finally, the diode ideality factor (n) provides information on where in the cell most recombinations are taking place. These parameters can be related to the key steps of the photovoltaic effect in order to further our understanding of light absorption, charge carrier recombinations and electric losses. The resistances are used to study PV module degradation [Sharma 2014].

There are other models which include more diodes connected in parallel, these introduce two more parameters per diode, a I_0 and n, in order to obtain a better approximation of the cell's behavior at low irradiances. The increase in complexity when including more parameters is rather high when solving the diode equation in order to extract the parameters and the main advantages are not as impressive when working with a wide range of high irradiances. Because of this, the single-diode model is favored over its more detailed counterparts in many studies [Jordehi 2016].

Experimental Campaign and Extraction Methods

The PV module under study was a polycrystalline silicon, Aluminium Back Surface Field (Al-BSF), model CS6K-260|265|270|275P by Canadian Solar. It has 60 PV cells connected in series and a total area of 1650^{x}992 mm^2. It is located on the rooftop of the Pontificia Universidad Catolica del Peru's Physics Section building.

Figure 2. Pontificia Universidad Católica del Perú - Materials Science and Renewable Energy group's PV station

The methods employed to extract the parameters of the single-diode model rely on the experimental current-voltage (I-V) curve. This was obtained by connecting an I-V curve tracer to the PV module, its main component is a capacitor which allows us to quickly vary the voltage from 0 to its maximum value [Conde 2020]. After this procedure several pairs of current and voltage are obtained, which make up the I-V curve. The I-V tracer circuit is also capable of measuring the module's temperature, finally an EKO MS-80 pyranometer, inclined by the same amount as the PV modules (20 °), was used to obtain the irradiance at the beginning and end of the tracing [Conde 2020]. These were used to apply the filter for constant irradiance during I-V tracing described in Ishii et al. [Ishii 2011]. Then the average between initial and ending irradiance for the inclined pyranometer was taken. In this study a total of 500 I-V curves were used, these were selected in the 100 - 1000 W/m^2 range. The distribution was 50 curves at (100 ± 5) W/m^2, 50 at (200 ± 5) W/m^2, and so forth until reaching (1000 ± 5) W/m^2. The module temperature at the time of I-V curve tracing was also recorded and used in the calculations. The data was measured over the course of a year-long experimental campaign from May 2019 to April 2020.

This study also had access to I-V data from thin-film PV technologies, obtained thanks to our collaboration with the Universidad de Jaén (Spain). The I-V tracer used for this data was also based on a capacitor, it was combined with two Agilent 34411A multimeters to measure current and voltage.

The thin-film modules studied were:

- Hydrogenated amorphous silicon (a-Si:H)
- Copper Indium Selenide (CIS)
- Cadmium Telluride (CdTe)
- Amorphous silicon / micro-cristalline silicon tandem (a-Si/μ-Si)

These were studied by selecting a single I-V curve, measured at an irradiance of 1000 W/m^2 and air temperature of 25 ℃, for each technology.

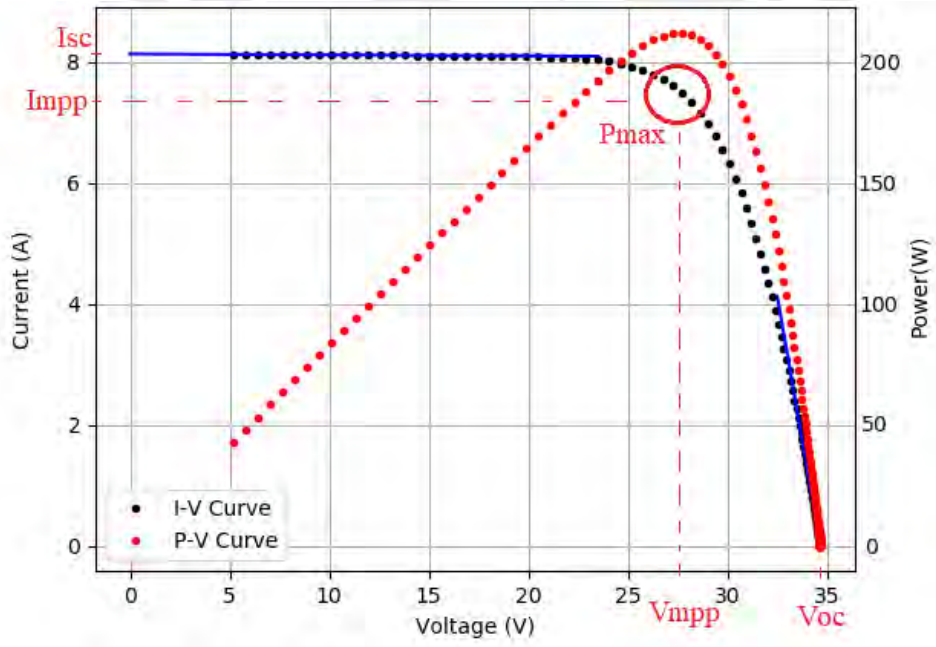

Figure 3. Experimental I-V curve and power-voltage curve for an Al-BSF module, showing key points and linear fits (in blue) applied to both extremes

The I-V curve is central to parameter extraction, so it is important to highlight some of its key points. The beginning of the curve has the highest value for current, it is known as the short-circuit current (I_{sc}). This current is achieved by using the I-V curve tracer's capacitor to set the voltage to zero. Another notable point is the opposite, the

voltage reaches its maximum value: the open-circuit voltage (V_{oc}) and current drops to zero. The values for voltage and current at the point where power output reaches its maximum (V_{mpp} and I_{mpp}, respectively) are essential as well. A couple of necessary quantities are obtained from the values of the slope of the I-V curve at the extremes. These are commonly obtained by applying a linear fit to the edges of the curve as shown in figure 3. The fit on the left is performed for points within 0-30 % of the V_{oc} and the fit on the right is for points within the 0-30 % of the maximum current measured. The linear fit on the left side can be used to extrapolate the curve and obtain the I_{sc} in case the I-V is incomplete due to measurement difficulties. The negative inverse of the slopes is related to the circuit's resistances, they are referred to as R_{so} and R_{sho}. All the values mentioned in this system of equations that can be solved to extract all five parameters [Fernández 2016].

$$R_{so} = -\left(\frac{dV}{dI}\right)_{V=V_{oc}} \tag{6}$$

$$R_{sho} = -\left(\frac{dV}{dI}\right)_{I=I_{sc}} \tag{7}$$

These linear fits work because the I-V curve is expected to behave linearly on both extremes when measured properly. A common issue when measuring the I-V curve is shading, sudden blocking of sunlight will result in step-like drops in the I-V curve. These must be filtered out as the linear approximation will not be accurate in this case and will lead to even greater errors when proceeding with the parameter extraction. The method chosen to filter them out is precisely with the linear fits, the error between the experimental curve and linear fit was calculated and a threshold value was chosen when no more errors could be found in the filtered I-V curves.

The single-diode model equation is nonlinear because of the exponential function, this forces us to either use a series of simplifications or a numerical algorithm to solve for

the five parameters. The methods selected for this study were the ones proposed by Phang et al.[Phang 1984], Blas et al.[Blas 2002] and Khan et al.[Khan 2013]. These methods were recommended by Montes-Romero et al.[Montes-Romero 2018] for their good balance between simplicity and success at extracting parameters. These analytical methods have advantages over numerical methods, mostly in the sense of ease of application. All three propose a series of assumptions about the magnitude of terms in the equations, relative to each other, with the objective of simplifying their solution. They all provide sets of formulas which can be used to calculate each parameter, these are easy to program and take little time to execute. Numerical methods on the other hand rely on computational algorithms that can prove complex to implement and come with a series of conditions necessary for them to function properly. All numerical algorithms will require a set of initial values for the five parameters, if these are not provided or they are not close enough to the real solution then the algorithm may not converge. Analytical methods may introduce some degree of error, but they still succeed at extracting the five parameters without straying too far away from the results obtained with numerical methods [Phang 1984].

Each method will provide a set of five electric parameters. These can be used along with the single-diode model equation (Equation 5) to simulate an I-V curve. Each method's modelled I-V curve can then be compared to the experimental I-V curve used originally to extract the parameters. The effectiveness of the extraction method is taken to be related to how well the simulated curve approximates the measured curve. A curve was generated for each method and for every experimental I-V curve, these modelled curves were then compared with the measurements to obtain a value for the extraction error. The Normalized Root Mean Square Error was used for this (Equation 21). Finally,

the comparison between methods was done by comparing the error value obtained in each method.

Phang et al. method

This analytical method provides an equation to calculate each of the single-diode model parameters. They can be solved using key points of the experimental I-V curve and parameters that have already been calculated:

$$R_{sh} = R_{sho} \tag{8}$$

$$n = \frac{V_{mpp} + R_{so} I_{mpp} - V_{oc}}{V_t \left[\ln\left(I_{sc} - \frac{V_{mpp}}{R_{sh}} - I_{mpp} \right) - \ln\left(I_{sc} - \frac{V_{oc}}{R_{sh}} \right) + \frac{I_{mpp}}{I_{sc} - \frac{V_{oc}}{R_{sh}}} \right]} \tag{9}$$

$$I_0 = \left(I_{sc} - \frac{V_{oc}}{R_{sh}} \right) \exp\left(-\frac{V_{oc}}{n V_t} \right) \tag{10}$$

$$R_s = R_{so} - \frac{n V_t}{I_0} \exp\left(-\frac{V_{oc}}{n V_t} \right) \tag{11}$$

$$I_{ph} = I_{sc} \left(1 + \frac{R_s}{R_{sh}} \right) + I_0 \left(\exp\left(\frac{I_{sc} R_s}{n V_t} \right) - 1 \right) \tag{12}$$

Blas et al. method:

An initial estimate for the series resistance followed by iteration was required at the beginning of this method, then R_{sh} and n were estimated using Equations 13 and 14. These values were then introduced into Equation 15 to recalculate R_s, this process is repeated until the values for these three parameters converge. Then the values for I_0 and I_{ph} can be calculated using Equations 16 and 17.

$$R_{sh} = R_{sho} - R_s \tag{13}$$

$$n = \frac{V_{mpp} + R_{so} I_{mpp} - V_{oc}}{V_t \ln\left[\frac{\left(I_{sc} - I_{mpp}\right)\left(1 + \frac{R_s}{R_{sh}}\right) - \frac{V_{mpp}}{R_{sh}}}{I_{sc}\left(1 + \frac{R_s}{R_{sh}}\right) - \frac{V_{oc}}{R_{sh}}}\right]} \tag{14}$$

$$R_s = \frac{R_{so}\left(\frac{V_{oc}}{nV_t} - 1\right) + R_{sho}\left(1 - \frac{I_{sc}R_{so}}{nV_t}\right)}{\frac{V_{oc} - I_{sc}R_{sho}}{nV_t}} \tag{15}$$

$$I_0 = \left(I_{sc}\left(1 + \frac{R_s}{R_{sh}}\right) - \frac{V_{oc}}{R_{sh}}\right)\exp\left(-\frac{V_{oc}}{nV_t}\right) \tag{16}$$

$$I_{ph} = I_0\left(\exp\left(\frac{V_{oc}}{nV_t}\right) - 1\right) + \frac{V_{oc}}{R_{sh}} \tag{17}$$

Khan et al. method:

This method uses Phang et al.'s Equation 8 for the shunt resistance. Two equations are provided for I_{ph}, one depends on I_{sc} while the other depends on V_{oc}. These can be identified as Equations 12 and 17 from the Phang et al. method and Blas et al. method respectively. It then introduces new equations to calculate the remaining parameters. In this work, Equation 12 was used for the silicon-based modules, then Equation 17 was chosen for the thin-film technologies following the suggestions made by Montes-Romero [Montes-Romero 2018].

$$R_s = R_{so} - \frac{V_{mpp} + R_{so} I_{mpp} - V_{oc}}{I_{mpp} + \left(\ln\left(I_{sc} - I_{mpp}\right) - \ln(I_{sc})\right)I_{sc}} \tag{18}$$

$$I_0 = \frac{nV_t}{R_{so} - R_s}\exp\left(-\frac{V_{oc}}{nV_t}\right) \tag{19}$$

$$n = \frac{V_{mpp} + R_s I_{mpp} - V_{oc}}{V_t\left(\ln\left(I_{sc} - I_{mpp}\right) - \ln(I_{sc})\right)} \tag{20}$$

Once the electric parameters had been obtained using each method, these were used to recreate the I-V curve. The methods' reliability was evaluated by comparing the

modelled curves to the experimental I-V curve through the calculation of their Normalized Root Mean Square Error (NRMSE) shown in Equation 21. In this equation, N is the number of pairs of experimental and modelled points used in the calculation. $I_{\text{Modelled}}(V)_i$ is the value for current calculated using the extracted parameters at a given voltage, $I_{\text{Measured}}(V)_i$ is the value measured for current at that same voltage. Finally, the I_{sc} is the short-circuit current extracted from the I-V experimental curve, it is used to normalize the value for error [Montes-Romero 2018].

$$NRMSE = 100 \times \sqrt{\frac{1}{N}\sum_{i=1}^{N}\left(\frac{I_{Modelled}(V)_i - I_{Measured}(V)_i}{I_{SC}}\right)^2} \tag{21}$$

I-V Curve Modelling Results and Error Comparison

The methods of Phang et al., Blas et al. and Khan et al. were able to extract the parameters with enough success to reproduce an Al-BSF's experimental I-V curve. Figure 4 shows how the modelled I-V curves overlap with each other and the measured data, showing that all three methods can be applied to this technology. In order to obtain a more detailed view of the difference in each method, we must look at the values for NRMSE obtained and how these changed with irradiance.

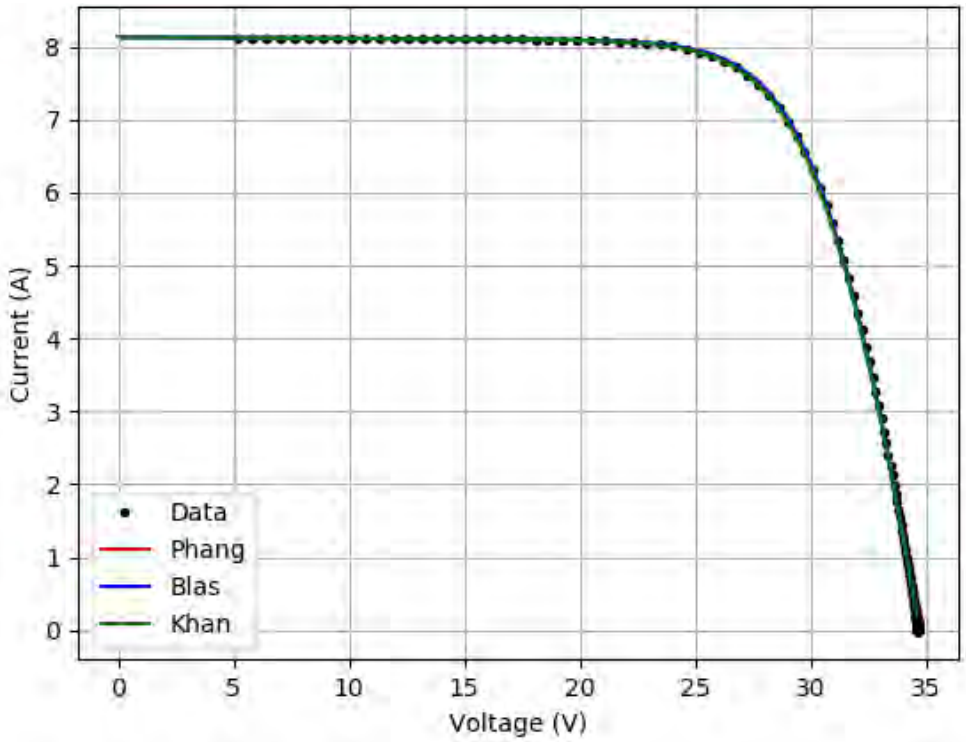

Figure 4. Experimental and modelled I-V curves for the Al-BSF module

Looking at each method separately allows to find out how the fitting error behaves with changes in irradiance. In order to compare NRMSE values obtained at different irradiances, boxplots of each group were created. In figures 5-7, each boxplot shows the distribution of NRMSE values for all I-V curves in each irradiance. Figure 5 shows how the error obtained when modelling the I-V curve using the Phang et al. method decreased as irradiance increased. The dispersion of NRMSE values also became smaller as irradiance increased. Both observations suggest that the parameters extracted with the Phang et al. method allow for better approximations of the I-V curve at higher irradiances.

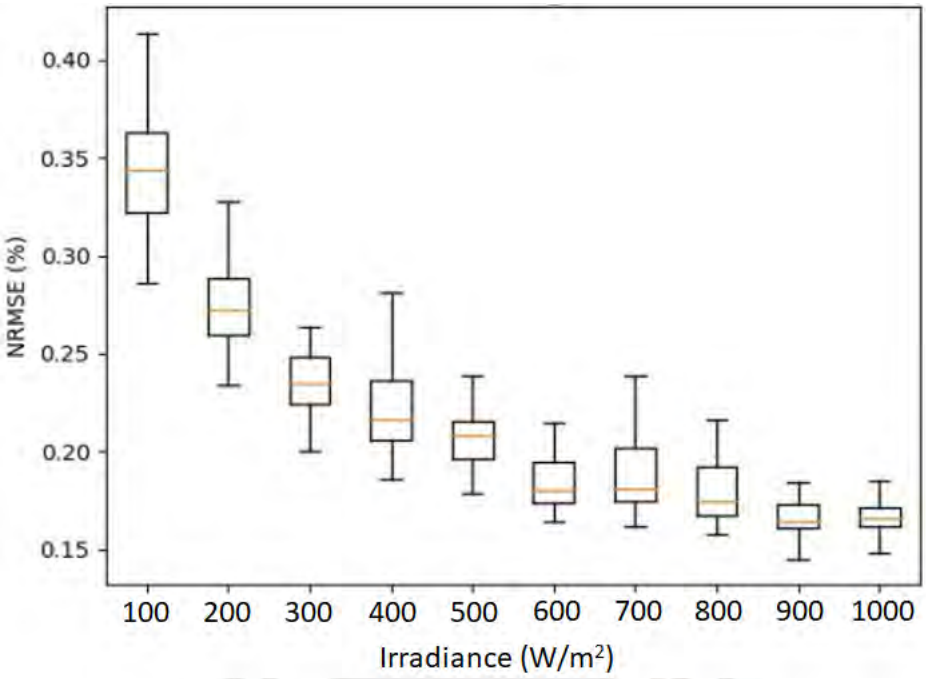

Figure 5. Boxplots of curve fitting error for every irradiance using the Phang et al. method

Figure 6 shows how the Blas et al. method gave similar results to the previous method, reproducing the same behavior of decreasing NRMSE median and dispersion as irradiance increased.

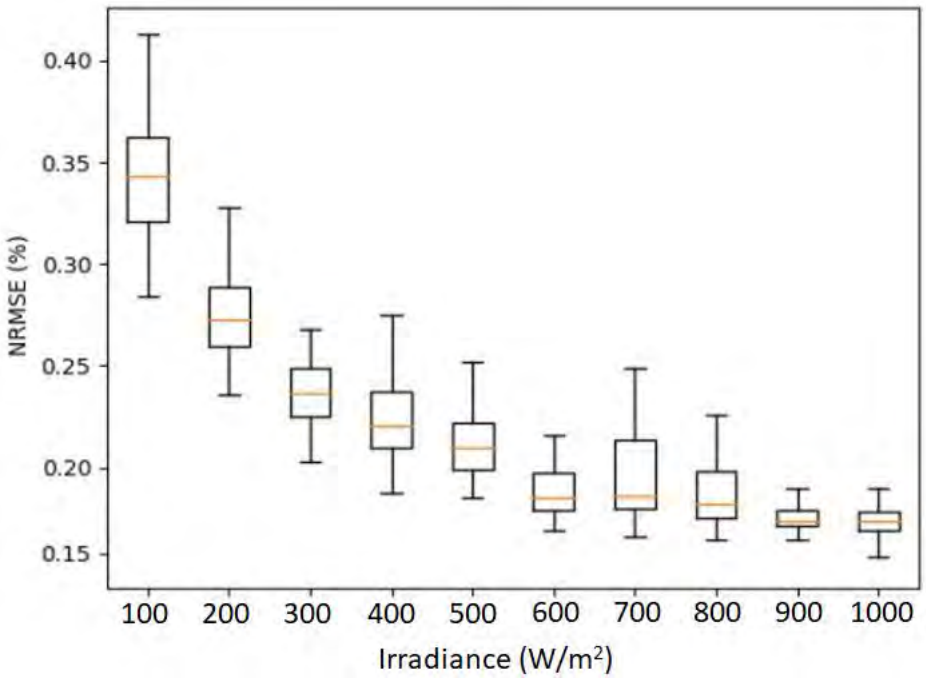

Figure 6. Boxplots of curve fitting error for every irradiance using the Blas et al. method

The method proposed by Khan et al. showed a different pattern with respect to changes in irradiance. Figure 7 shows how there is an initial decrease in NRMSE but as soon as irradiance reaches 200W/m^2, the error obtained becomes stable and does not vary noticeably with increasing irradiance. The values for NRMSE obtained with the Khan et al. method are also larger than in the other two methods, with the biggest NRMSE surpassing 0.70% while Phang et al. and Blas et al. never exceeded 0.45%.

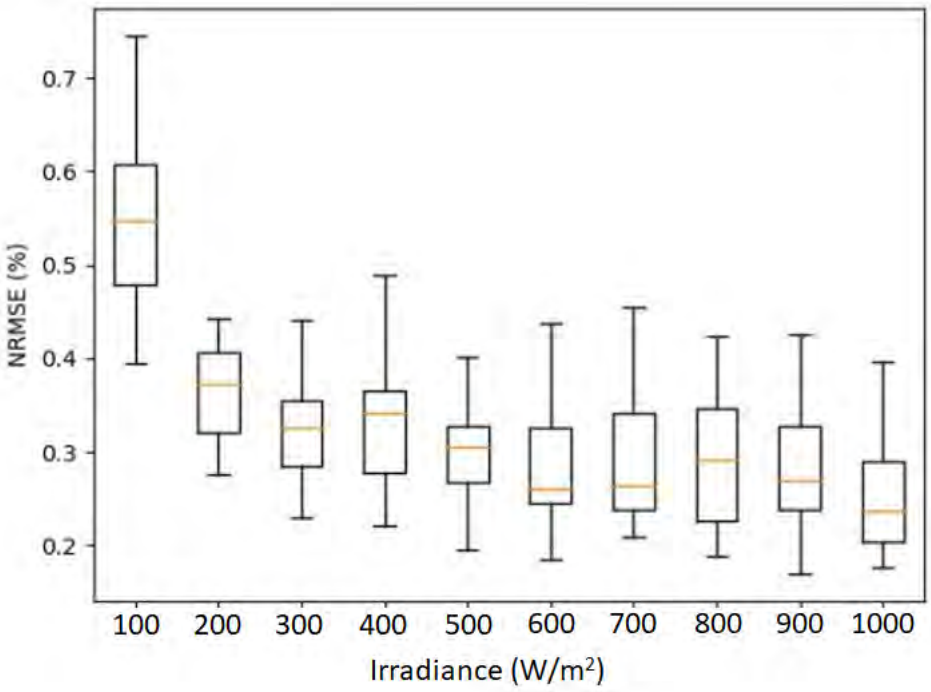

Figure 7. Boxplots of curve fitting error for every irradiance using the Khan et al. method

All the irradiances are summarized in a single graph using figure 8, which shows the boxplots for each method next to each other to compare how well they performed overall. The graph shows how the errors of Phang et al. and Blas et al. were indistinguishable in these tests, while the Khan et al. method obtained both a larger median and dispersion.

It should be noted that the behavior shown primarily in figures 5 and 6 might be due to the definition of NRMSE used, which normalizes the error using the I_{sc}. This parameter is known to be linear with respect to irradiance so its use in the denominator

might lead to a decreasing NRMSE when comparing curves at different irradiances. Different ways of normalizing the error could be attempted in the future but fall outside of the scope of this study.

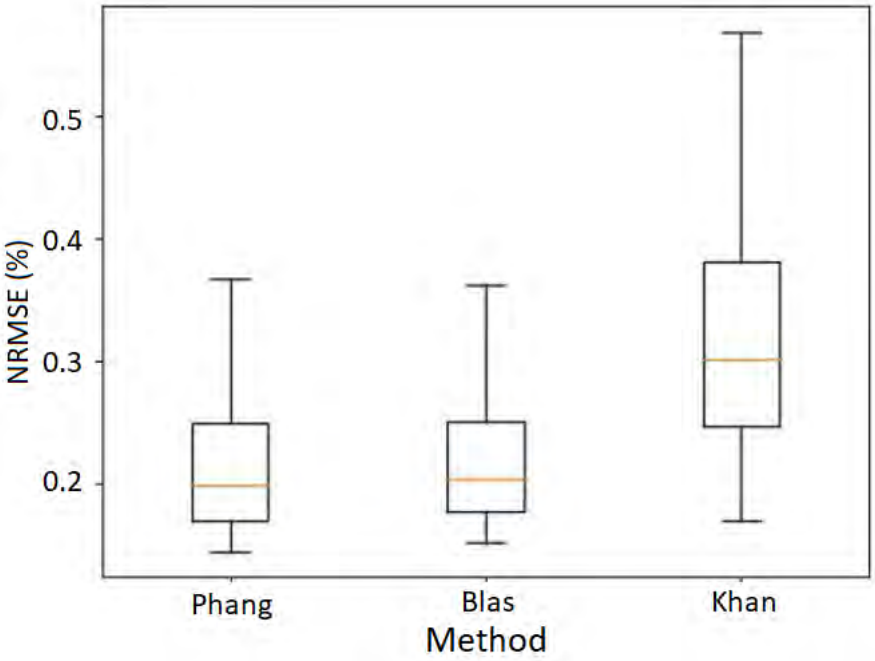

Figure 8. Boxplots for each method, using I-V curves at every irradiance

The extraction methods were also applied to four thin-film technologies. The method proposed by Blas et al. was not applied to thin-film technologies due to the chronological development of this work in which Phang et al. and Khan et al. were studied first.

The difference in success at extracting the five parameters from the single-diode model was evaluated visually by presenting the modelled curves next to the measured I-V curve in figures 9-12. As well as quantitatively by calculating the NRMSE and plotting it in figure 13.

Figures 9-12 show the Phang et al. method succeeding in creating a modelled I-V curve capable of approximating the experimental curve for every technology under study. The method proposed by Khan et al. shows mixed results, it overestimates the I_{sc} for the

a-Si / μ-Si and a-Si modules but achieves better fitting for the CdS/CdTe and CIS modules. A key difference in these technologies is the shape of their experimental I-V curves, the first two technologies show steeper and less linear behaviour in the proximity of the I_{sc}. This fact makes those technologies' data look less like the Al-BSF module's I-V curve, which had a horizontal and nearly flat section near the I_{sc}. This difference could lead to worse linear approximations when applying the methods to thin-film technologies which in turn leads to greater error when extracting the five parameters. The method proposed by Phang et al. uses an equation (Equation 12) for I_{ph} which is more related to the I_{sc} than the equation proposed by Khan et al. (Equation 17). This way Phang's method makes sure the modelled curve stays close to the measured I_{sc} when voltage is low.

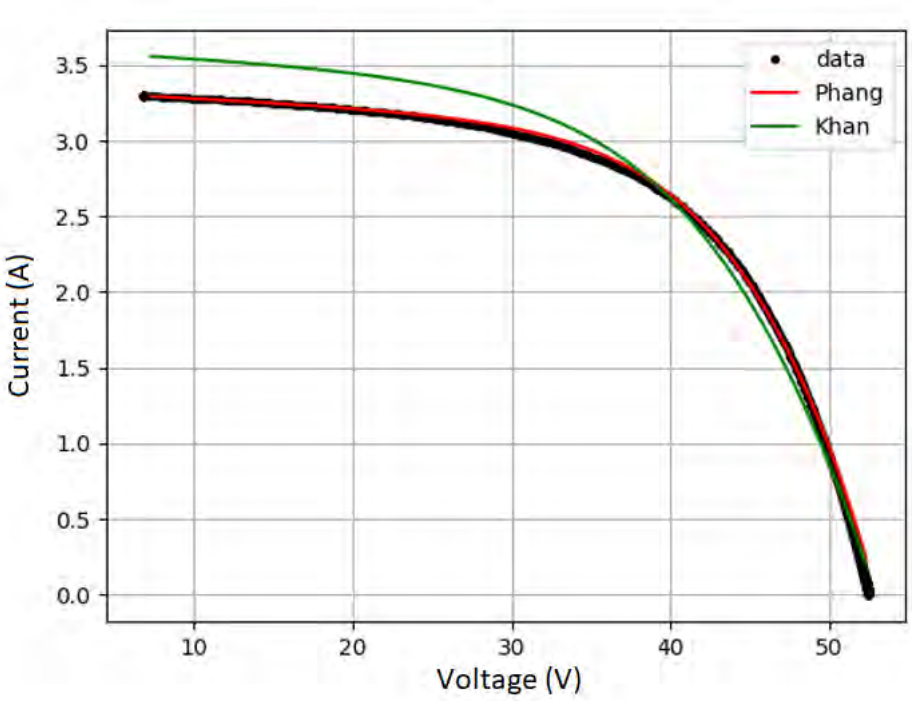

Figure 9. Experimental and modelled I-V curves for the a-Si / μ-Si module

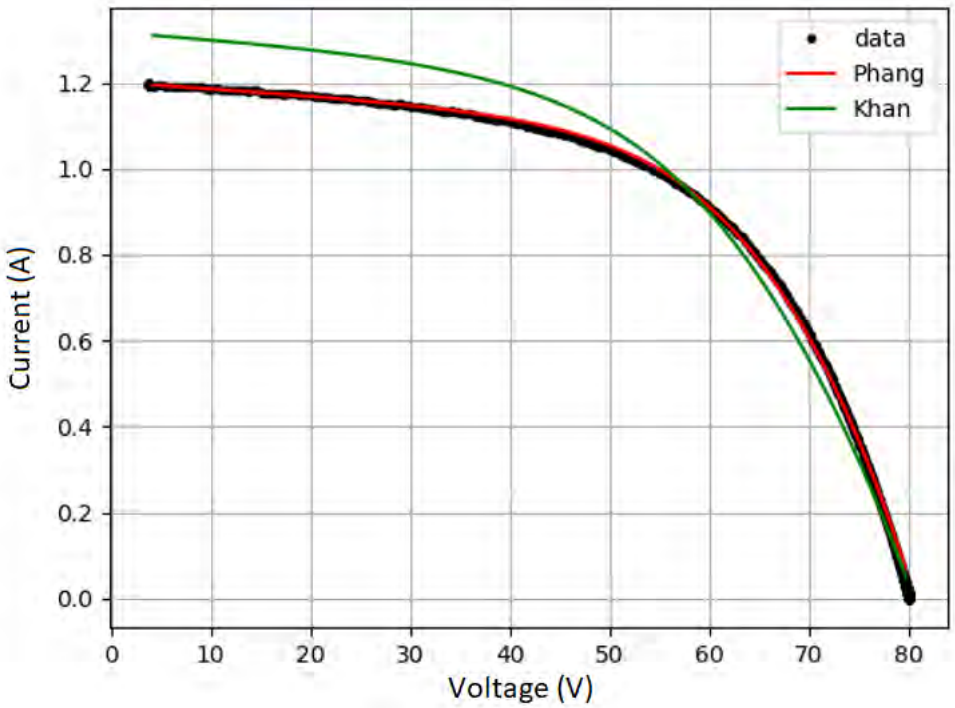

Figure 10. Experimental and modelled I-V curves for the a-Si:H module

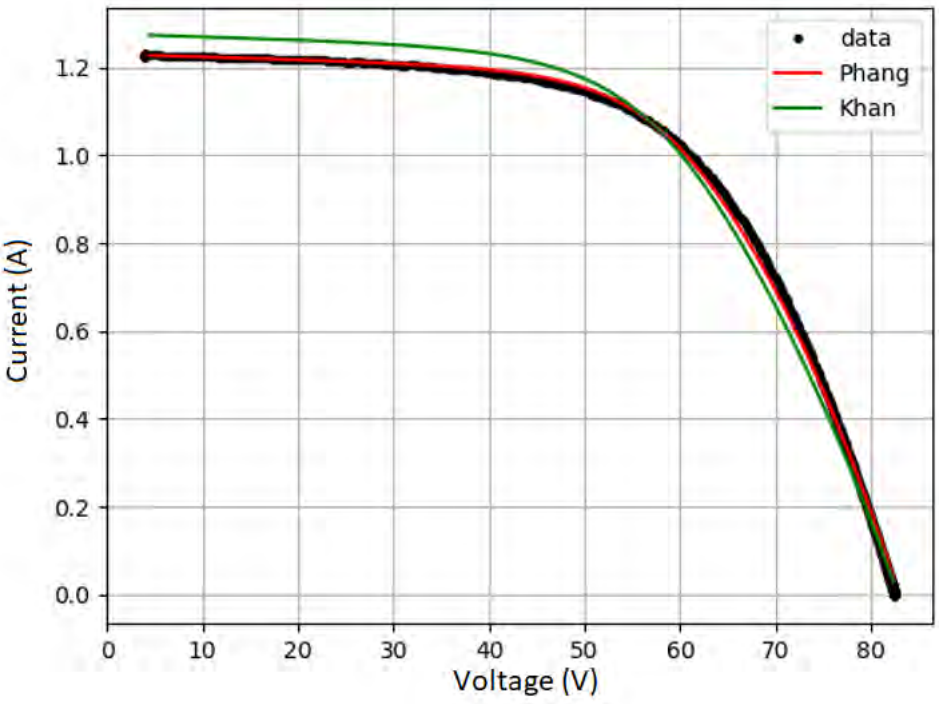

Figure 11. Experimental and modelled I-V curves for the CdS/CdTe module

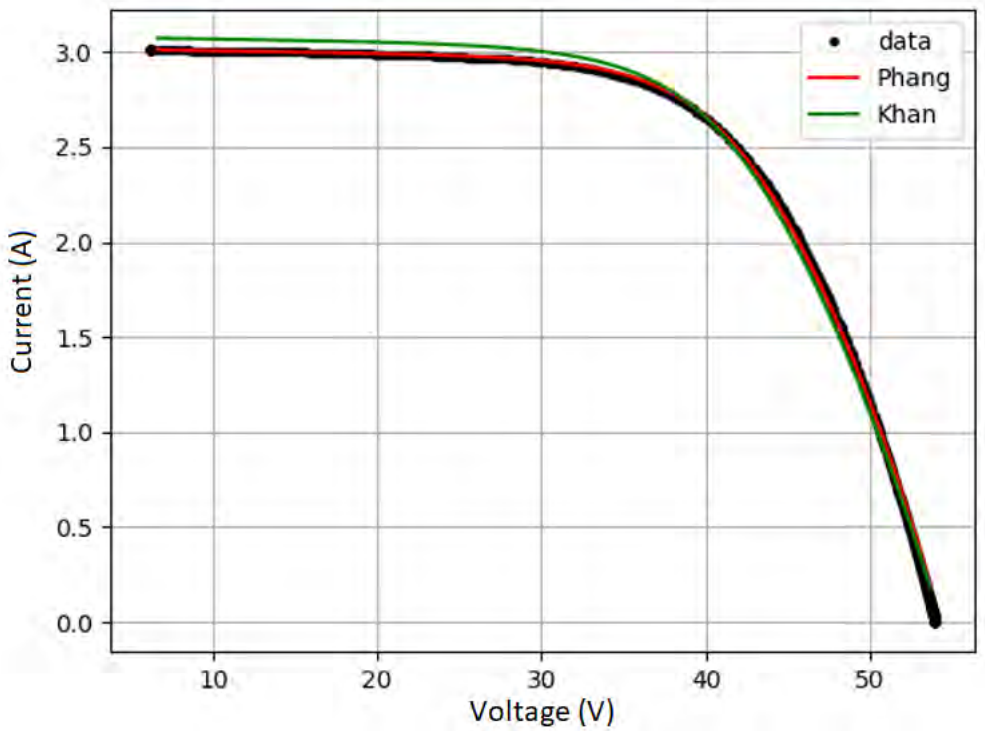

Figure 12. Experimental and modelled I-V curves for the CIS module

Figure 13 shows how the error behaved with each technology. Phang et al.'s method has consistent low fitting error with every PV technology, while Khan's method exhibits a much higher error for some of the thin-film modules. This increased error in Khan's method is most apparent in the a-Si:H and a-Si/μ-Si modules, which showed the least linear behavior close to the I_{sc} and where the biggest overestimations of the experimental I-V curve can be observed.

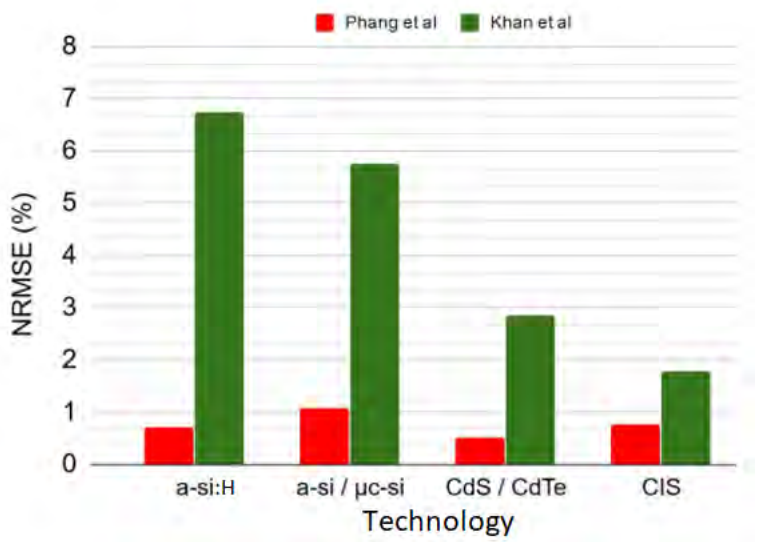

Figure 13. Error obtained for each method across the different PV technologies

Summary and Conclusion

We set out to compare the Phang et al., Blas et al. and Khan et al. parameter extraction methods with the objective of finding out which one gave the lowest I-V curve fitting error. After testing them under different irradiance conditions and across several technologies we found out that the method proposed by Phang et al. obtained the best results according to the NRMSE. This is clear from the low error in the Al-BSF multiple irradiance measurements as well as in the thin-film module comparisons. The Blas et al. method also obtained low error across the 100-1000 W/m^2 irradiance range for the Al-BSF module. The Khan et al. method managed to maintain higher error than the other two methods in the silicon-based module tests, when applied to thin-films it showed mixed results but it always had a bigger error than Phang et al.

Future studies could investigate different ways of normalizing the error to remove the dependence on I_{sc} which might influence the NRMSE's behavior with irradiance. Otherwise, new ways of evaluating the parameter extraction that eliminate the need for NRMSE calculations could be tested. Thin-films require more detailed studies that take

more I-V curves into consideration, preferably at multiple irradiances, so the results can be generalized more easily.

From the results obtained in this study, we conclude that the method proposed by Phang et al. excels in versatility when it comes to extracting the parameters from the single-diode model. Given that it has succeeded in extracting parameters at multiple irradiances and using several PV technologies, while maintaining a low median NRMSE of 0.2 % for silicon and 0.5-1.1 % for thin-film modules. Phang et al.'s error was comparable to Blas et al.'s for the Al-BSF module (median NRMSE of 0.21 %), it also maintained lower error than Khan et al.'s for every circumstance (median NRMSE of 0.30 % for silicon and 1.77-6.73 % for thin-films).

Acknowledgements

Special thanks to the PUCP-MatER group and the University of Jaen's IDEA group for their continued assistance. Financial support provided by the Peruvian National Fund for Scientific and Technological Development (FONDECYT) through Contract N° 124-2018-FONDECYT.

Publications

Part of this work was published in a May 2020 issue of the UNI's TECNIA magazine. It was also presented at the XXVI Simposio Peruano de Energía Solar (SPES 2019) and at the Jornadas Peruanas de Energía Solar (JOPES 2020).

References

Blas, M., Torres, J., Prieto, E., & García, A., (2002). Selecting a suitable model for characterizing photovoltaic devices. *Renewable Energy*, 25(3), 371–380. doi:10.1016/s0960-1481(01)00056-8

Ciulla, G., Lo Brano, V., Di Dio, V., Cipriani, G., (2014). A comparison of different one-diode models for the representation of I–V characteristic of a PV cell. *Renewable and Sustainable Energy Reviews*, 32, 684-696, https://doi.org/10.1016/j.rser.2014.01.027.

Conde, L., Montes-Romero, J., Carhuavilca, A., Perich, R., Guerra, J., Sevillano, M., Calsi, B., Angulo, J., De la Casa, J., Palomino, J., (2020). Puesta en marcha de un laboratorio para la caracterización de tecnologías fotovoltaicas a sol real bajo las condiciones climáticas de Lima. *TECNIA*, 30(1), 80-89. https://doi.org/10.21754/tecnia.v30i1.835

Fernández, E. F., Montes-Romero, J., de la Casa, J., Rodrigo, P., Almonacid, F., Comparative study of methods for the extraction of concentrator photovoltaic module parameters. (2016). *Solar Energy*, 137, 413-423, https://doi.org/10.1016/j.solener.2016.08.046.

Ghani, F., Rosengarten, G., Duke, M., Carson, J.K.,(2014). The numerical calculation of single-diode solar-cell modelling parameters. *Renewable Energy*, 72, 105-112, https://doi.org/10.1016/j.renene.2014.06.035.

Ishii, T., Otani, K., & Takashima, T. (2011). Effects of solar spectrum and module temperature on outdoor performance of photovoltaic modules in round-robin measurements in Japan. *Progress in Photovoltaics: Research and Applications*, *19*(2), 141–148. https://doi.org/10.1002/pip.995

Jordehi, A., (2016). Parameter estimation of solar photovoltaic (PV) cells: A review, *Renewable and Sustainable Energy Reviews*, 61, 354-371, https://doi.org/10.1016/j.rser.2016.03.049.

Khan, F., Baek, S.-H., Park Y., Kim J. H., (2013) Extraction of diode parameters of silicon solar cells under high illumination conditions. *Energy Conversion and Management*, vol. 76, pp. 421–429. https://doi.org/10.1016/j.enconman.2013.07.054

Kumar, M., Kumar, A. (2017). Performance assessment and degradation analysis of solar photovoltaic technologies: A review. *Renewable and Sustainable Energy Reviews*. 78. 554-587. DOI: 10.1016/j.rser.2017.04.083.

Montes-Romero, J., Almonacid, F., Theristis, M., de la Casa, J., Georghiou, G. E., Fernández, E. F. (2018). Comparative analysis of parameter extraction techniques for the electrical characterization of multi-junction CPV and m-Si technologies. *Solar Energy*, 160, 275–288. https://doi.org/10.1016/j.solener.2017.12.011

Ogbomo, O., Amalu, E., Ekere, N., Olagbegi, P.O., (2017). A review of photovoltaic module technologies for increased performance in tropical climate, *Renewable and Sustainable Energy Reviews*, 75, 1225-1238, https://doi.org/10.1016/j.rser.2016.11.109.

Perich, R., Sevillano-Bendezú, M., Montes-Romero, J., Conde, L., Angulo, J., De la Casa, J., Palomino, J. (2020). Estudio de los métodos analíticos para la extracción de parámetros eléctricos de módulos fotovoltaicos de capas delgadas. *TECNIA*, *30*(1), 53-58. https://doi.org/10.21754/tecnia.v30i1.851

Phang, J. C. H., Chan, D. S. H., Phillips, J. R., (1984). Accurate analytical method for the extraction of solar cell model parameters. *Electronics Letters*, vol. 20, no. 10, pp. 406-408.

Sharma, V., Sastry, O. S., Kumar, A., Bora, B., & Chandel, S. S. (2014). Degradation analysis of a-Si, (HIT) hetro-junction intrinsic thin layer silicon and m-C-Si solar photovoltaic technologies under outdoor conditions. *Energy*, 72, 536–546. doi:10.1016/j.energy.2014.05.078

Wang, Y., Zhou, S., Huo, H., (2014). Cost and CO2 reductions of solar photovoltaic power generation in China: Perspectives for 2020, *Renewable and Sustainable Energy Reviews*, 39, 370-380, https://doi.org/10.1016/j.rser.2014.07.027.